

# First spectroscopic investigation of the 4d transition metal monocarbide MoC

Dale J. Brugh, Theodore J. Ronningen, and Michael D. Morse  
*Department of Chemistry, University of Utah, Salt Lake City, Utah 84112*

(Received 5 June 1998; accepted 7 August 1998)

The first optical spectroscopic investigation of MoC has revealed a complicated vibronic spectrum consisting of about 35 bands between 17 700 and 24 000  $\text{cm}^{-1}$ . Analysis has shown the ground state to be the  $\Omega=0^+$  spin-orbit component of a  $^3\Sigma^-$  state that derives from a  $10\sigma^2 11\sigma^2 5\pi^4 2\delta^2$  configuration. The  $X^3\Sigma_0^-$  rotational constant for  $^{98}\text{Mo}^{12}\text{C}$  was determined to be  $B_0=0.553\,640 \pm 0.000\,055 \text{ cm}^{-1}$ , giving  $r_0=1.687\,719 \pm 0.000\,084 \text{ \AA}$ . Consideration of spin-uncoupling effects in the  $X^3\Sigma^-$  state requires that this value be revised to  $r_0=1.6760 \text{ \AA}$ , which represents our best estimate of the true Mo-C bond length. Spectroscopic constants were also extracted for six other major isotopic modifications of MoC in this mass resolved experiment. All rotationally resolved transitions were found to originate from the ground state and terminate in electronic states with  $\Omega=1$ . An attempt is made to classify the observed transitions into band systems, to rationalize the complexity of the spectrum, and to understand the bonding from a molecular orbital point of view.

© 1998 American Institute of Physics. [S0021-9606(98)01342-7]

## I. INTRODUCTION

In comparison to the available gas phase spectroscopic data for the 3d transition metal monocarbides, of which only FeC,<sup>1-3</sup> CoC,<sup>4,5</sup> and NiC (Ref. 6) have been studied in detail as isolated gas phase entities, the 4d carbides are becoming a well characterized group of molecules. The first of the 4d monocarbides, YC,<sup>7</sup> was also the first transition metal carbide to be investigated in a jet-cooled experiment. There it was found that YC possesses a  $^4\Pi_i$  ground state deriving from the  $10\sigma^2 11\sigma^1 5\pi^3 12\sigma^1$  configuration. Spectra for the next 4d monocarbide, ZrC, have been recorded, and a  $^1\Sigma^+$  ground state has been determined.<sup>8</sup> Simard and co-workers<sup>9</sup> have collected optical spectra for the next carbide in line, NbC, and established its ground electronic state as  $^2\Delta_r$ , deriving from a  $10\sigma^2 11\sigma^2 5\pi^4 2\delta^1$  configuration. Clearly, one of the interesting results of these studies has been the observation that it becomes more favorable to occupy the  $2\delta$  orbital between YC and NbC.

Postponing discussion of MoC for the moment, TcC is the next 4d carbide, but no experimental work has yet been reported for this diatomic. Considerably more is known about RuC, the carbide to the right of TcC in the 4d series. Two high temperature studies in the early 1970s provided the first spectroscopic data on RuC,<sup>10,11</sup> but these investigations produced molecules that were too hot to allow the ground state electronic symmetry to be established. More recent work conducted in this group<sup>12</sup> has established the ground state of RuC as  $^1\Sigma^+$  deriving from the  $10\sigma^2 11\sigma^2 5\pi^4 2\delta^4$  configuration. It appears that the addition of three electrons on moving from NbC to RuC simply fills the  $2\delta$  orbital. Next in the 4d metal-carbide series is another well studied molecule, RhC.<sup>13</sup> Its ground state has been established as  $10\sigma^2 11\sigma^2 5\pi^4 2\delta^4 12\sigma^1$ ,  $^2\Sigma^+$ . The  $12\sigma$  orbital is occupied in RhC for the first time upon leaving YC. Finally, PdC has recently been produced and interrogated,<sup>14</sup> and the ground

state has been established as possessing  $\Omega=0$ . The ground electron configuration and term from which this  $\Omega$  value arises is still uncertain at this writing. With the addition of the current work on MoC, the ground states of seven of the 4d metal monocarbides are now well characterized by gas phase optical spectroscopy, in contrast to just three for the 3d carbides.

In the first reported work on gaseous MoC, Gupta and Gingerich<sup>15</sup> conducted a Knudsen effusion mass spectrometric study of the products obtained upon heating Mo in a graphite furnace. Employing molecular parameters estimated from the relevant oxide data available at the time and their mass spectrometric equilibrium data, they determined the bond dissociation energy of MoC to be 4.95 eV using the third law method. In a recent *ab initio* study of MoC that included relativistic corrections, Shim and Gingerich<sup>16</sup> have calculated the ground state of MoC to be  $10\sigma^2 11\sigma^2 5\pi^4 2\delta^2$ ,  $^3\Sigma^-$  with  $\omega_e=997 \text{ cm}^{-1}$  and  $r_e=1.688 \text{ \AA}$ . As might be expected, these recently calculated molecular parameters differ from those used by Gupta and Gingerich in their original determination of the MoC bond strength because the bonding in the carbides is considerably different than in the oxides, the model for their original estimates. This has led Shim and Gingerich to revise the experimental MoC bond strength to  $D_0(\text{MoC})=5.01 \pm 0.13 \text{ eV}$ . Apart from these two studies, we are unaware of any other work on MoC, experimental or theoretical.

In the following section we present a brief discussion of the experimental methods employed to record the spectra of MoC. Section III presents the spectroscopic results obtained for MoC. Now that TcC, AgC, and CdC are the only 4d transition metal carbides to receive no spectroscopic attention, it is possible to rationalize the bonding trends in the 4d transition metal carbides, and this is accomplished in Sec.

IV. Section V concludes the paper with a summary of our most important results.

## II. EXPERIMENT

A timely and brief description of the R2PI spectrometer and general experimental procedure can be found in the publication detailing our recent investigation of FeC.<sup>3</sup> Details can also be found in a number of earlier publications.<sup>17,18</sup> Only a brief sketch of the conditions relevant to this study of molybdenum monocarbide will be given here.

Laser ablation (Continuum Powerlite 8000 Nd:YAG; 532 nm, 3 mJ/pulse) of a Mo target in the presence of methane in helium (3% CH<sub>4</sub>) followed by expansion into vacuum through a 3 cm long, 2 mm diam channel produced MoC in high yield. Backed by a gas reservoir pressure of 120 psig, the ensuing supersonic expansion effectively cooled the contents of the molecular beam before it was skimmed and allowed to enter the extraction region of a Wiley–McLaren time-of-flight mass spectrometer. There, R2PI spectroscopy was performed by sequentially exposing the molecular beam to the output of a pulsed tunable dye laser (Molelectron DL-222) pumped by the frequency tripled output of a Nd:YAG laser (Quantel Model 581-C) and subsequently to the output of an excimer laser (Lambda Physik, Compex 200) operating on an ArF gas filled at 6.42 eV. For low resolution survey scans at a resolution of about 0.6 cm<sup>-1</sup>, approximately 5–8 mJ of energy was available per laser pulse. In order to resolve the rotational structure of individual bands of MoC, higher resolution radiation (0.04 cm<sup>-1</sup>) was generated by the insertion of an air spaced étalon into a vacuum tight portion of the oscillator cavity of the same dye laser. The laser frequency was then pressure tuned over a range of about 15 cm<sup>-1</sup> with Freon-12 (CCl<sub>2</sub>F<sub>2</sub>, DuPont). Approximately 1–2 mJ of this radiation was generally available for rotationally resolved studies.

Calibration of the rotationally resolved scans was accomplished by collecting the fluorescence of iodine from 17 700 cm<sup>-1</sup> to 20 000 cm<sup>-1</sup> and comparing this to the atlas of Gerstenkorn and Luc.<sup>19</sup> Following a correction for the error in this atlas<sup>20</sup> and for the Doppler shift due to the velocity of the molecular beam relative to the excitation laser radiation, the measured rotational line positions are believed to have an absolute accuracy of ±0.02 cm<sup>-1</sup>. For calibration of line positions to the blue of 19 450 cm<sup>-1</sup>, isotopically pure <sup>130</sup>Te was heated to either 510 °C or 650 °C to collect the absorption spectrum of the equilibrium concentration of Te<sub>2</sub> present in a sealed absorption cell. This spectrum was compared to the atlas of Cariou and Luc<sup>21</sup> to obtain an absolute frequency match. After a correction for the Doppler shift, the reported line positions for these bands are again believed to be accurate to ±0.02 cm<sup>-1</sup>.

Excited state lifetime data were collected by the time delay technique in which the delay between excitation and ionization of the molecular species is systematically varied to map out the excited state population of that species as a function of this delay. The exponential decay is then fit to one of several decay models to extract an excited state lifetime.

## III. RESULTS

Because of its seven naturally occurring and abundant isotopes (<sup>92</sup>Mo, 14.84%; <sup>94</sup>Mo, 9.25%; <sup>95</sup>Mo, 15.92%; <sup>96</sup>Mo, 16.68%; <sup>97</sup>Mo, 9.55%; <sup>98</sup>Mo, 24.13%; <sup>100</sup>Mo, 9.63%),<sup>22</sup> Mo containing species are difficult to study spectroscopically unless it is possible to separate the spectrum of each isotope from that of the others. In an optical study, this can be done most reliably and reproducibly in a mass resolved R2PI experiment. Even with mass resolution, however, mass coincidences can occur that have the potential to complicate the identification of the carrier of a spectrum, especially when a molecule possesses several isotopic modifications. No serious complications occurred in this study because careful calibration of the mass spectrometer allowed the mass of the carrier to be determined without ambiguity, eliminating other possible candidates for the carrier of the observed spectra such as MoO and MoCH. Careful attention was given to the mass spectrum during low resolution survey scans for signs of any MoCH transition, which would have been most obvious in the gaps of the MoC mass pattern at masses 105 amu and 111 amu. No enhancement was ever observed; indeed, no transition was observed in any other Mo containing hydrocarbon. Care was also taken to ensure that no contamination from MoO was present at the masses of coincidence between MoC and MoO (108 amu, 110 amu, and 112 amu), especially in the region of this study that was known from previous work to possess MoO transitions.<sup>23</sup> No transitions that could be ascribed to MoO were observed, however. It is quite certain that the bands reported in this paper are exclusively due to the isotopes of MoC.

### A. General features

The spectral region between 17 700 cm<sup>-1</sup> and 24 000 cm<sup>-1</sup> was found to consist of about 35 bands. Of these, 24 were sufficiently intense to be probed with rotational resolution, but four did not yield to analysis, and one additional band could not be reliably calibrated. For none of the rotationally resolved bands was there any evidence of hyperfine splitting or broadening of the rotational lines for the isotopes with nuclear spin, <sup>95</sup>Mo<sup>12</sup>C and <sup>97</sup>Mo<sup>12</sup>C.

In the fitting of each band, integer values of *J* were used in the assignment of each line, and the first observed lines were always *R*(0), *Q*(1), and *P*(2). This is indicative of an Ω = 1 ← Ω = 0 transition, and it applied to every rotationally resolved band. This implies that the ground state possesses Ω = 0 and that a number of excited states with Ω = 1 exist. For all rotationally resolved bands, satisfactory residuals in the fits of the line positions could only be obtained by the inclusion of lambda doubling in the Ω = 1 upper state. Because each transition was found to terminate in an Ω = 1 electronic state and originate from an Ω = 0 state, the lambda doubling energy is proportional to *J*'(*J*' + 1).<sup>24</sup> With these items in mind, the formulas used to fit the rotational line positions of each rotationally resolved band can be written succinctly following the standard conventions<sup>25,26</sup> as

$$\nu_{P,R/Q} = \nu_0 + [B'J'(J'+1) - B''J''(J''+1)] \mp \frac{1}{2}q'J'(J'+1), \quad (1)$$

where  $q'$  is the upper state lambda doubling parameter. This definition of  $q'$  assumes that the upper state is a  $^3\Pi_1$  level,<sup>25</sup> as is suggested in Sec. IV D.

It can be established that only a single  $\Omega''=0$  level is present rather than an  $\Omega''=0^\pm$  pair because the rotational lines were observed as single, undoubled  $R(J)$ ,  $Q(J)$ , and  $P(J)$  transitions. This observation further suggests that the ground state is a  $\Sigma$  state. The lower state rotational levels must therefore possess  $e$  parity because the only  $\Omega''=0$  states that can be generated from the reasonable candidates for the ground state ( $^1\Sigma^+$  and  $^3\Sigma^-$ ) are  $\Omega=0^+$ . Selection rules dictate that  $e$  levels can connect only with  $e$  levels in  $P$  and  $R$  branches, requiring the use of  $-\frac{1}{2}q'J'(J'+1)$  in Eq. (1).<sup>26</sup>  $Q$ -branch lines that originate from an  $e$  level must terminate on an  $f$  level, requiring the use of  $+\frac{1}{2}q'J'(J'+1)$  in Eq. (1). Fits of measured line positions yielded values of the parameters  $\nu_0$ ,  $B'$ ,  $B''$ , and  $q'$  for each band. The fact that the lower level involved in each transition must possess  $e$  parity allows the branch labels to be written as  $P_e(J)$ ,  $R_e(J)$ , and  $Q_{fe}(J)$ .

Extracting these four spectroscopic parameters for each band, along with the excited state lifetime, was straightforward. A complete list of all line positions, fit residuals, and the extracted spectroscopic constants determined in this study of MoC can be obtained from the Physics Auxiliary Publication Service (PAPS) of the American Institute of Physics or from the author (M.D.M.).<sup>27</sup> Grouping the observed transitions according to electronic state proved more difficult. No regular and repeating band spacings that would indicate a progression were ever found. As an alternative approach, an attempt was made to find patterns in the isotope shifts and rotational constants among all the rotationally resolved bands. If the isotope shifts for individual bands are plotted as a function of transition energy, the shifts for bands belonging to a progression are expected to lie approximately on a line for the first several vibrational levels as long as the anharmonicity is not too large. If vibrational levels with sufficiently large  $v'$  are observed, anharmonicity will cause the isotope shifts to curve away from a straight line as  $v'$  increases. Moreover, the slope of the expected line in a region that should be approximately linear can be calculated using the known values of the reduced masses of the isotopomers and estimates of  $\omega'_e$ ,  $\omega'_e x'_e$ ,  $\omega''_e$ , and  $\omega''_e x''_e$ . Often a figure such as this, which displays measured isotope shifts as a function of transition energy on the same plot as lines of calculated isotope shifts for various vibrational assignments, is used to determine the absolute vibrational numbering of the bands in an identified progression. Here, the band systems have not yet been found, and the plot is used to initially identify them. For MoC, this proved to be partially successful.

During data collection, care was taken to ensure that data for  $^{98}\text{Mo}^{12}\text{C}$  and  $^{100}\text{Mo}^{12}\text{C}$  were as clean and complete as possible to provide a consistent set of isotope shifts for all bands of MoC. In retrospect, this choice was probably not the best because the expected shift for this pair of isotopes [ $\nu(^{100}\text{Mo}^{12}\text{C})-\nu(^{98}\text{Mo}^{12}\text{C})$ ] is only on the order of  $-10\text{ cm}^{-1}$  for  $v' < 12$ . Its use as an interpretive tool is therefore severely compromised by any isotopically dependent perturba-

tions that may be present. Such perturbations can readily cause the observed isotope shifts to deviate from the calculated shifts in an unknown manner, leading to a relatively large change in a relatively small number. The larger the isotope shift, the less the relative effect of the perturbation. If the isotope shift is made large enough, such as would be the case between  $^{98}\text{Mo}^{12}\text{C}$  and  $^{98}\text{Mo}^{13}\text{C}$ , the perturbation becomes washed out in comparison to the shift, and the shifts become a more meaningful indicator of which bands belong to which systems. The large isotope shifts observed upon substitution of  $^{13}\text{C}$  for  $^{12}\text{C}$  undoubtedly played an important role in the identification of the band systems in NbC,<sup>9</sup> and the small shifts observed in this study of MoC have undoubtedly contributed to the difficulty associated with grouping bands into systems.

At any rate, isotopically enriched  $^{13}\text{CH}_4$  was not available for these studies, and isotope shifts had to be gleaned from the naturally abundant isotopes. Moreover, the shift between  $^{100}\text{Mo}^{12}\text{C}$  and  $^{98}\text{Mo}^{12}\text{C}$  had to be used if as many bands as possible (17) were to be compared simultaneously. For a given band system and any isotopic pair, the expected slope of the line composed of measured isotope shifts ( $\Delta\nu$ ) as a function of transition frequency ( $\nu$ ) can be readily calculated from the expression for the vibrational term energy

$$G(v) = \omega_e(v + \frac{1}{2}) - \omega_e x_e(v + \frac{1}{2})^2 \quad (2)$$

and the isotopic relations  $\omega'_e(^{100}\text{Mo}^{12}\text{C}) = \rho \omega'_e(^{98}\text{Mo}^{12}\text{C})$  and  $\omega'_e x'_e(^{100}\text{Mo}^{12}\text{C}) = \rho^2 \omega'_e x'_e(^{98}\text{Mo}^{12}\text{C})$ ,<sup>24</sup> where  $\rho$  is defined as the square root of the ratio of the reduced mass of  $^{98}\text{Mo}^{12}\text{C}$  to that of  $^{100}\text{Mo}^{12}\text{C}$ . The resultant expression giving the expected slope between  $v'=2$  and  $v'=0$  is

$$(\rho - 1) \left[ \frac{\omega'_e - 3(\rho + 1)\omega'_e x'_e}{\omega'_e - 3\omega'_e x'_e} \right]. \quad (3)$$

If anharmonicity is ignored either because it is small in comparison to  $\omega'_e$  or because its value is not precisely known, the expected slope reduces to  $\rho - 1$ . Anharmonicity will certainly cause the slope to deviate from this value, but the value of  $\rho - 1$  provides a useful starting point for the analysis. In the case of  $^{100}\text{Mo}^{12}\text{C}$  and  $^{98}\text{Mo}^{12}\text{C}$ , the expected initial slope of a plot of  $\Delta\nu$  vs  $\nu$  is  $-0.00109$ , if the isotope shift ( $\Delta\nu$ ) is defined as  $\nu(^{100}\text{Mo}^{12}\text{C}) - \nu(^{98}\text{Mo}^{12}\text{C})$ . Though the fact that shifts lie along such a line cannot prove that the bands to which they correspond belong to a progression, it at least provides possibilities and supporting evidence, and here it allowed the tentative identification of three systems in MoC.

## B. The ground $X\Omega=0$ state

As has already been argued in Sec. III A, the lower state of each rotationally resolved transition is  $\Omega=0$  which most likely derives from a  $\Sigma$  state. Furthermore, all the fitted lower state rotational constants for any one isotope are very similar, indicating that the state from which these transitions originate is the same for each band. Because these experiments were carried out in a supersonically cooled molecular beam, it is virtually certain that this  $\Omega=0$  state is the ground state of MoC. It would be shocking if it were not. To arrive at the best estimate of  $B''$  for each isotope, a weighted average of all the individually determined  $B''$  values from each

TABLE I. MoC weighted average ground state rotational constants and bond lengths.<sup>a</sup>

| Isotope                           | $B_0$ (cm <sup>-1</sup> ) | $r_0$ (Å) <sup>b</sup> | Bands |
|-----------------------------------|---------------------------|------------------------|-------|
| <sup>92</sup> Mo <sup>12</sup> C  | 0.557 54(10)              | 1.687 79(15)           | 9     |
| <sup>94</sup> Mo <sup>12</sup> C  | 0.556 164(59)             | 1.687 796(90)          | 12    |
| <sup>95</sup> Mo <sup>12</sup> C  | 0.555 471(57)             | 1.687 839(86)          | 14    |
| <sup>96</sup> Mo <sup>12</sup> C  | 0.554 820(60)             | 1.687 842(91)          | 16    |
| <sup>97</sup> Mo <sup>12</sup> C  | 0.554 357(60)             | 1.687 576(92)          | 16    |
| <sup>98</sup> Mo <sup>12</sup> C  | 0.553 640(55)             | 1.687 719(84)          | 17    |
| <sup>100</sup> Mo <sup>12</sup> C | 0.552 563(73)             | 1.687 50(11)           | 17    |

<sup>a</sup>The 1 $\sigma$  error limit in the last two decimal places is shown in parentheses following each constant.

<sup>b</sup>The bond lengths are calculated assuming that the  $B_0$  values are directly related to the moment of inertia of the molecule. That is, no spin-uncoupling effects have been considered. These values most likely do not represent the true Mo–C bond length.

fitted band was taken. All fitted values of  $B''$  were used in each weighted average except for the values determined for the band near 21 241 cm<sup>-1</sup>. These values were considered suspect because the fitted free spectral range of the étalon used in the data calibration was quite different from that determined for the same étalon in nearby spectral regions. This likely occurred because there were few calibrated Te<sub>2</sub> absorption lines available in this region for an absolute frequency reference. Otherwise, all data were used. The weighted average values of  $B_0$  for the  $X\Omega=0$  state of MoC for each isotope are provided in Table I along with the bond lengths to which they convert and the number of bands used to determine the value of  $B_0$ . All the data suggest that the ground state of MoC is sufficiently removed from other states such that it remains relatively unperturbed. Even when severe perturbations prevented the fitting of a band with Eq. (1), it was possible to extract a value of  $B''$  quite close to those in Table I via combination differences.<sup>24</sup>

Although bond lengths have been extracted for each of the isotopes of MoC, the rotational constants in Table I may not be directly related to the moment of inertia of the molecule because of spin-uncoupling interactions with the  $\Omega=1$  component of the ground  $^3\Sigma^-$  term. This possibility is explored more deeply in Sec. IV. For now, it is sufficient to say that it must be kept in mind that the bond lengths reported in Table I may require revision when the  $\Omega=1$  component of the  $X^3\Sigma^-$  state is experimentally characterized and analyzed.

### C. The [18.6] $\Omega=1 \leftarrow X\Omega=0$ system

At approximately 18 612 cm<sup>-1</sup> is the origin of a three member progression possessing an irregular vibrational spacing. The initial assignment of the three bands at 18 612 cm<sup>-1</sup>, 19 453 cm<sup>-1</sup>, and 20 333 cm<sup>-1</sup> as the 0–0, 1–0, and 2–0 bands, respectively, of the same system was accomplished with a plot of isotope shifts ( $\Delta\nu$ ) vs transition frequencies ( $\nu$ ). The slope of the best line through the data for these three bands when the <sup>98</sup>Mo<sup>12</sup>C to <sup>100</sup>Mo<sup>12</sup>C isotope shift is used is nearly double that calculated from Eq. (3), but it is clear that the three data points lie on the same line. A similar result is found when other isotopic pairs are used. Other evidence strongly suggests that these three bands belong to the same system. The fact that the isotope shift for the first member of the progression is nearly zero ( $-0.0502 \pm 0.0023$  cm<sup>-1</sup>) is good evidence that the 18 612 cm<sup>-1</sup> band is an origin band. As mentioned, the isotope shift for the 19 453 cm<sup>-1</sup> band is larger than expected, but it is not unreasonable for a 1–0 band. It is initially disturbing that the measured excited state lifetime for the <sup>98</sup>Mo<sup>12</sup>C isotope of the 19 453 cm<sup>-1</sup> band is 2.5  $\mu$ s while those of the bands assigned as 0–0 and 2–0 are on the order of 800 ns. In Table II, however, it can be found that the measured lifetime (660

TABLE II. Spectroscopic constants determined for three isotopes of each band in identified band systems of MoC.

| State             | $v' - v''$        | Isotope                           | $\nu_0$ (cm <sup>-1</sup> )       | $B'_v$ (cm <sup>-1</sup> ) | $\tau$ ( $\mu$ s) | $\Delta\nu_0$ (cm <sup>-1</sup> ) <sup>a</sup> | $q'$ (cm <sup>-1</sup> ) |              |
|-------------------|-------------------|-----------------------------------|-----------------------------------|----------------------------|-------------------|--|--------------------------|--------------|
| [18.6] $\Omega=1$ | 0–0               | <sup>97</sup> Mo <sup>12</sup> C  | 18 611.989 1(21)                  | 0.503 95(33)               | 0.839(52)         | +0.036 5(24)                                   | 0.000 82(13)             |              |
|                   |                   | <sup>98</sup> Mo <sup>12</sup> C  | 18 611.952 6(12)                  | 0.503 822(97)              | 0.7210(50)        | ...  | 0.000 852(52)            |              |
|                   |                   | <sup>100</sup> Mo <sup>12</sup> C | 18 611.902 4(20)                  | 0.502 66(16)               | ...               | -0.050 2(23)                                   | 0.000 736(86)            |              |
|                   | 1–0               | <sup>97</sup> Mo <sup>12</sup> C  | 19 454.080 7(27)                  | 0.507 34(35)               | 0.659(36)         | +1.044 3(71)                                   | -0.009 00(15)            |              |
|                   |                   | <sup>98</sup> Mo <sup>12</sup> C  | 19 453.036 4(65)                  | 0.494 83(68)               | 2.54(22)          | ...  | -0.026 34(48)            |              |
|                   |                   | <sup>100</sup> Mo <sup>12</sup> C | 19 451.082 0(34)                  | 0.516 31(48)               | ...               | -1.954 4(74)                                   | -0.002 46(24)            |              |
|                   | 2–0               | <sup>97</sup> Mo <sup>12</sup> C  | 20 335.006 4(26)                  | 0.517 86(24)               | 1.17(14)          | +2.163 0(33)                                   | -0.012 41(12)            |              |
|                   |                   | <sup>98</sup> Mo <sup>12</sup> C  | 20 332.843 4(21)                  | 0.518 41(29)               | 0.897(19)         | ...  | -0.012 092(84)           |              |
|                   |                   | <sup>100</sup> Mo <sup>12</sup> C | 20 328.723 9(22)                  | 0.521 97(55)               | ...               | -4.119 4(31)                                   | -0.011 25(16)            |              |
| [20.7] $\Omega=1$ | 0–0               | <sup>97</sup> Mo <sup>12</sup> C  | 20 700.266 7(20)                  | 0.510 15(17)               | ...               | +0.579 9(29)                                   | -0.001 172(70)           |              |
|                   |                   | <sup>98</sup> Mo <sup>12</sup> C  | 20 699.686 8(21)                  | 0.509 82(17)               | 0.365(8)          | ...  | -0.000 996(76)           |              |
|                   |                   | <sup>100</sup> Mo <sup>12</sup> C | 20 698.554 7(22)                  | 0.508 49(24)               | ...               | -1.132 1(30)                                   | -0.000 806(86)           |              |
|                   | 1–0               | <sup>97</sup> Mo <sup>12</sup> C  | 21 539.429 3(29)                  | 0.503 55(32)               | ...               | +1.276 8(55)                                   | -0.001 19(16)            |              |
|                   |                   | <sup>98</sup> Mo <sup>12</sup> C  | 21 538.152 4(47)                  | 0.502 75(39)               | 0.259(8)          | ...  | -0.000 82(17)            |              |
|                   |                   | <sup>100</sup> Mo <sup>12</sup> C | 21 535.650 9(27)                  | 0.502 45(29)               | ...               | -2.501 5(54)                                   | -0.001 54(16)            |              |
|                   | [22.5] $\Omega=1$ | 0–0                               | <sup>97</sup> Mo <sup>12</sup> C  | 22 521.145 0(39)           | 0.493 98(40)      | ...  | +0.778 6(48)             | 0.008 74(28) |
|                   |                   |                                   | <sup>98</sup> Mo <sup>12</sup> C  | 22 520.366 5(28)           | 0.495 54(31)      | 0.296(6)                                       | ...                      | 0.009 16(16) |
|                   |                   |                                   | <sup>100</sup> Mo <sup>12</sup> C | 22 519.122 0(21)           | 0.495 82(28)      | ...  | -1.244 4(35)             | 0.009 29(16) |
| 1–0               |                   | <sup>97</sup> Mo <sup>12</sup> C  | 23 324.694 6(17)                  | 0.484 43(17)               | ...               | +1.132 3(37)                                   | -0.006 576(78)           |              |
|                   |                   | <sup>98</sup> Mo <sup>12</sup> C  | 23 323.562 3(33)                  | 0.483 42(37)               | 0.437(19)         | ...  | -0.007 14(19)            |              |
|                   |                   | <sup>100</sup> Mo <sup>12</sup> C | 23 321.368 4(40)                  | 0.481 76(47)               | ...               | -2.194 0(52)                                   | -0.009 46(20)            |              |

<sup>a</sup>The isotope shift is reported as the band origin of the isotopic modification relative to that of <sup>98</sup>Mo<sup>12</sup>C:  $\nu_0(^i\text{Mo}^{12}\text{C}) - \nu_0(^{98}\text{Mo}^{12}\text{C})$ .

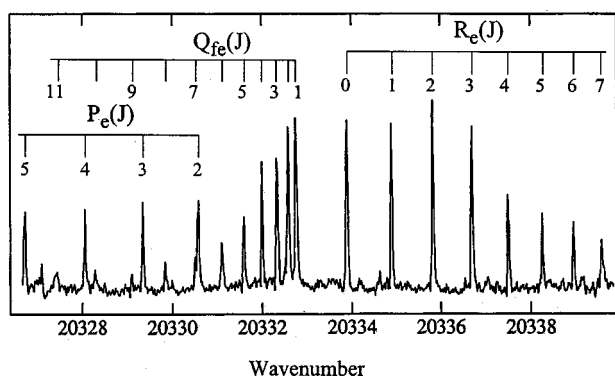


FIG. 1. Rotationally resolved spectrum of the  $^{98}\text{Mo}^{12}\text{C}$   $[18.6]\Omega=1\leftarrow X\Omega=0^+ 2-0$  band. The rotational structure obtained upon exciting the  $v'=2$  level of the  $[18.6]\Omega=1$  state from the  $v''=0$  level of the ground state of  $^{98}\text{Mo}^{12}\text{C}$  at an excitation laser resolution of  $0.04\text{ cm}^{-1}$  is shown with the branch labels and the  $J$  numbering of each line. The  $Q_{fe}$  branch fans out to lower energy and no abrupt band head is observed, indicating a slight increase in bond length upon excitation. The small gap between the  $R_e$  and  $Q_{fe}$  branches indicates an  $\Omega=1\leftarrow 0$  transition.

ns) for the  $^{97}\text{Mo}^{12}\text{C}$  isotope of the  $19\,453\text{ cm}^{-1}$  band is considerably different than that for the  $^{98}\text{Mo}^{12}\text{C}$  isotope. This value is much closer to the lifetimes measured for the other bands in this progression. Clearly, the  $^{98}\text{Mo}^{12}\text{C}$  isotope is perturbed in some way. The lambda doubling parameters also indicate that something is amiss with the  $^{98}\text{Mo}^{12}\text{C}$  isotope. If it is assumed that the  $^{98}\text{Mo}^{12}\text{C}$  isotope of the  $19\,453\text{ cm}^{-1}$  band is perturbed one must compare the  $B'_v$  values of other isotopes to determine if the expected  $B'_v$  trend is observed. For none of the isotopes do the  $B'_v$  values exhibit the steady decrease with  $v'$  that is expected. On the contrary, a steady increase with  $v'$  is observed for  $^{97}\text{Mo}^{12}\text{C}$  and  $^{100}\text{Mo}^{12}\text{C}$ , implying an unphysical negative value for  $\alpha_e$ . Despite this inconsistency in the measured  $B'_v$  values, the pattern of isotope shifts and the measured lifetimes seem to confirm that these transitions terminate in the same excited electronic state. The intensities of the bands as observed in low resolution spectra are consistent with the Franck-Condon pattern expected in a transition in which the bond length changes only moderately upon excitation. The similarity of the measured values of  $q'$  and their patterned decrease as  $v'$  increases for all the isotopes, except  $^{98}\text{Mo}^{12}\text{C}$ , is also supportive of their assignment as  $0-0$ ,  $1-0$ , and  $2-0$  bands of a single progression.

The irregular spacing of the bands precludes the determination of meaningful values of  $\omega'_e$  and  $\omega'_e x'_e$ , but the numbers can readily be calculated to be  $\omega'_e=802.4\text{ cm}^{-1}$  and  $\omega'_e x'_e=-19.4\text{ cm}^{-1}$ . No error limits are associated with these values because three band origins uniquely determine  $\omega'_e$  and  $\omega'_e x'_e$ . Assuming that the upper states are not perturbed in such a way as to make the  $B$ -values unrelated to the moment of inertia, the decrease in the upper state rotational constants relative to those of the ground state indicates a slight increase in bond length upon excitation. The rotationally resolved spectrum of the  $2-0$  band of this progression is shown in Fig. 1, and there it can be seen that the  $Q_{fe}$  branch fans out to lower energy as is expected if the  $B$ -value decreases upon excitation. The  $R_e$  branch is approaching a

band head, but it does not reach it before the intensity of the lines drops to zero.

#### D. The remaining possible band systems

The assignment of bands to a progression when there are only two members is tentative at best, especially when using the technique that was used in assignment of the  $[18.6]\Omega=1\leftarrow X\Omega=0$  system. After all, any two points describe a perfect line. A greater reliance must be made on the actual measured slope of the line intersecting the  $(\nu, \Delta\nu)$  data points for the bands in question. With these caveats in mind, a second likely system is that defined by the bands located near  $20\,700\text{ cm}^{-1}$  and  $21\,538\text{ cm}^{-1}$ . The slope of the line through these  $(\nu, \Delta\nu)$  data points is  $-0.001\,63$ , a number which is as close to the expected value of  $-0.001\,09$  as could be obtained. The upper state rotational constants decrease from the lower energy band to the higher as expected, and the lifetimes of the two upper states are similar,  $365\text{ ns}$  and  $259\text{ ns}$ , respectively. These two bands yield  $\Delta G'_{1/2}=838.47\pm 0.51\text{ cm}^{-1}$ , a reasonable value for an electronically excited transition metal carbide.

Also lending support to this assignment is the fact that the first of these bands is nearly twice as intense as the second. Based on the total lack of bands  $900\pm 200\text{ cm}^{-1}$  to the red of the  $20\,700\text{ cm}^{-1}$  band, there seem to be no prior members of this progression. It then seems reasonable to assign these bands as the  $0-0$  and  $1-0$  bands of the  $[20.7]\Omega=1$  system. The isotope shifts are certainly larger than would be expected for  $0-0$  and  $1-0$  bands, but, then again, only one band in the entire spectral region covered in this study, the  $18\,611\text{ cm}^{-1}$  band, possesses an isotope shift of the magnitude expected for a  $0-0$  band. It seems unreasonable to think that the entire spectrum of MoC that has been observed would contain just a single origin band; therefore, it is necessary to accept the idea that origin bands have isotope shifts larger than expected (near  $1\text{ cm}^{-1}$ ) in this molecule. Data for three isotopes of each band in this system are tabulated in Table II.

The third possible band system consists of two bands located near  $22\,520\text{ cm}^{-1}$  and  $23\,323\text{ cm}^{-1}$ . The slope of the line through the  $(\nu, \Delta\nu)$  data points for these two bands ( $-0.001\,18$ ) is quite close to the expected value of  $-0.001\,09$ . A value of  $\Delta G'_{1/2}=803.1958\pm 0.0043\text{ cm}^{-1}$  can be extracted from these two bands, a value which is, again, reasonable for an electronically excited transition metal carbide. The lifetimes are similar and the rotational constants decrease as expected from the lower energy band to the higher energy band. The intensity pattern in the low resolution survey scan is again as expected with the first band more intense than the second. Also as before, there is nothing  $800\text{ cm}^{-1}$  to the red of the  $22\,520\text{ cm}^{-1}$  band to suggest that it is anything but an origin band, despite the fact that its isotope shift is over  $1\text{ cm}^{-1}$ . This band is therefore assigned as the  $0-0$  band of the  $[22.5]\Omega=1$  system, and the  $23\,323\text{ cm}^{-1}$  band as the  $1-0$ . Data for this system are also listed in Table II. The rotationally resolved spectra for bands in both of these tentatively assigned band systems appear very similar to that shown in Fig. 1.

TABLE III. Spectroscopic constants<sup>a</sup> of unclassified MoC bands.

| $\nu_0$ (cm <sup>-1</sup> ) | $B'$ (cm <sup>-1</sup> ) | $\tau$ ( $\mu$ s) | $\Delta\nu_0$ (cm <sup>-1</sup> ) <sup>b</sup> |
|-----------------------------|--------------------------|-------------------|--|
| 20 094.437 9(11)            | 0.515 82(11)             | 0.313(30)         | -1.537 7(16)                                   |
| 20 332.843 4(21)            | 0.518 41(29)             | 0.897(19)         | -4.119 4(31)                                   |
| 20 390.020 9(36)            | 0.454 06(45)             | 5.50(50)          | -4.875 3(51)                                   |
| 20 736.405 7(44)            | 0.508 48(51)             | 2.140(10)         | -0.890 0(85)                                   |
| 20 901.682 9(19)            | 0.506 79(18)             | 0.296(13)         | -1.066 3(27)                                   |
| 21 596.401 0(36)            | 0.472 42(42)             | 0.623(20)         | -0.784 7(63)                                   |
| 22 066.552 0(15)            | 0.504 79(15)             | 0.526 0(90)       | -1.574 7(20)                                   |
| 22 187.243 6(27)            | 0.506 75(30)             | 0.233 0(80)       | -1.923 1(45)                                   |
| 22 338.281(10)              | 0.492 0(28)              | 0.554 0(60)       | -1.983(10)                                     |
| 22 319.114 4(34)            | 0.496 48(45)             | 0.356 0(10)       | -0.751 6(41)                                   |
| 22 844.520 0(21)            | 0.507 34(24)             | 0.202 0(50)       | -2.182 1(34)                                   |

<sup>a</sup>The  $1\sigma$  error limits for each parameter in the last two decimal places is shown in parentheses.

<sup>b</sup>The isotope shift is reported as the band origin of the <sup>100</sup>Mo<sup>12</sup>C species relative to that of the <sup>98</sup>Mo<sup>12</sup>C species.

### E. Unassigned resolved bands

The three band systems discussed above account for only seven of the observed bands. This leaves 13 rotationally resolved and analyzed bands unclassified by electronic state as well as four bands that could not be fully analyzed because of extensive perturbations. The analyzed bands that cannot be classified share some general features in common. All have upper states with  $\Omega=1$ , an exasperating fact that contributes substantially to the difficulty in classification. In addition, they all possess isotope shifts [ $\nu_0(^{100}\text{Mo}^{12}\text{C})-\nu_0(^{98}\text{Mo}^{12}\text{C})$ ] that are, on average, between  $-1.5$  and  $-2.0$  cm<sup>-1</sup>. The lifetimes are generally less than 1  $\mu$ s except for a few bands whose lifetime are quite long. For instance, the upper states of the bands near 20 736 cm<sup>-1</sup> and 20 390 cm<sup>-1</sup> have lifetimes of 2.14  $\mu$ s and 5.5  $\mu$ s, respectively. As with the bands assigned to systems, the unassigned bands all display a decrease in  $B$ -value upon excitation. For some this change is moderate, but for a few it is fairly dramatic. The band located near 20 395 cm<sup>-1</sup>, for instance, displays a decrease in  $B$ -value that converts to a bond length increase of 0.18 Å. Most often the change is less than 0.1 Å. Of course, this assumes that the fitted  $B$ -values are directly related to the moment of inertia and that they are not seriously distorted by the perturbations that are apparently present throughout the spectrum of MoC.

In addition to the three band systems tentatively identified in Table II, at least two more excited states must be present. One of these possesses a long lifetime and has a bond length considerably longer than that of the ground state. The others have bond lengths that are more nearly the same as the ground state and shorter lifetimes. Undoubtedly there are strong interactions between the excited  $\Omega=1$  states in this region, leading to a scrambled vibronic spectrum that is not readily organized into band systems. Spectroscopic data for the <sup>98</sup>Mo<sup>12</sup>C isotope of each of the unclassified but analyzed bands are listed in Table III, and data for the remaining isotopes are available from the Physics Auxiliary Publication Service (PAPS) (Ref. 27) or from the author (M.D.M.) upon request. The PAPS tables also include the line positions gathered at high resolution for bands that were not found to fit well because of perturbations.

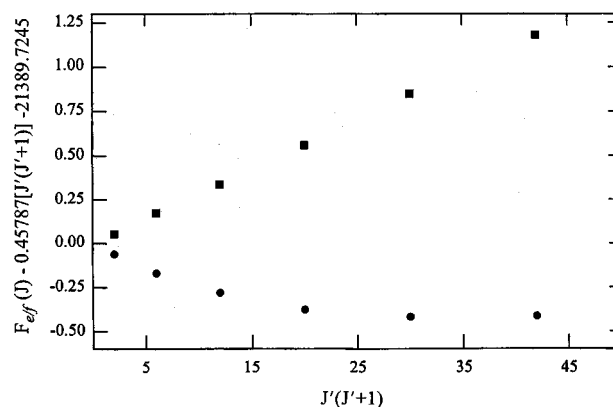


FIG. 2. Term energies of the  $e$  and  $f$  levels of the <sup>98</sup>Mo<sup>12</sup>C 21 390 cm<sup>-1</sup> band. The term energies  $F_e - 0.457 87[J'(J'+1)] - 21 389.724 5$  and  $F_f - 0.457 87[J'(J'+1)] - 21 389.724 5$  are shown. The upper set of data points shown as closed squares are the  $F_f$  levels. These are linear as a function of  $J'(J'+1)$ . The lower set of data points shown as closed circles are the  $F_e$  levels. These deviate from a straight line severely as  $J$  increases, indicating a perturbation by an  $\Omega=0^+$  state that lies below 21 390 cm<sup>-1</sup>.

### F. Evidence of an excited $\Omega=0$ state

From an  $\Omega=0$  ground state, only  $\Omega=0$  and 1 excited states can be observed. As reported above, numerous  $\Omega=1$  states were spectroscopically accessed in the region probed, but no  $\Omega=0 \leftarrow \Omega=0$  transitions were found. Though no  $\Omega=0 \leftarrow 0$  transition was observed, there is evidence that an  $\Omega=0$  state exists near 21 400 cm<sup>-1</sup>. Its presence is manifested through its effect on the line positions of a nearby  $\Omega=1 \leftarrow 0$  transition that was rotationally resolved.

The rotationally resolved spectrum of the 21 390 cm<sup>-1</sup> band of <sup>98</sup>Mo<sup>12</sup>C appeared normal at first, but an attempt to fit the line positions to Eq. (1) led to unacceptably large residuals and to a ground state rotational constant that was considerably different than expected. When, instead, combination differences were taken between lines that terminate on the same upper state rotational level, the value of  $B''$  for this band was determined to be  $0.553 64 \pm 0.000 42$  cm<sup>-1</sup>. This value is numerically equal to the weighted average value of  $B''$  for <sup>98</sup>Mo<sup>12</sup>C that is tabulated in Table I. This is good evidence that this band originates from the ground state of MoC and that whatever perturbation is causing the poor fit to Eq. (1) can be entirely attributed to the upper state. Further insight into this band can be gained by plotting the term energies of the upper state  $e$  and  $f$  rotational levels,  $F_e(J)$  and  $F_f(J)$ , as a function of  $J(J+1)$ . Because the lambda doubling energy and the rotational energy for an  $\Omega=1$  state are proportional to  $J(J+1)$ , these term energies ought to lie along lines with different slopes. Such a plot is shown in Fig. 2. The term energies have been plotted about the average line between the two sets of term energies to allow the differences between them to be better discerned. It can be seen in Fig. 2 that the  $F_f$  term energies, shown in closed squares at the top of the figure, follow a straight line as expected from Eq. (1). The  $F_e$  term energies, however, deviate from a straight line, and it is now clear why the line positions collected to form Fig. 2 would not fit well to Eq. (1).

What is striking about Fig. 2 is that only the upper state  $e$  levels seem to be affected. For this to happen, the elec-

tronic state causing the perturbation must contain only  $e$  parity levels. This can only be true of  $\Omega=0^+$  states. Furthermore, because the  $e$  levels are seen to deviate in a positive direction from the expected line, it can be deduced that the perturbing  $\Omega=0^+$  state lies below the rotationally resolved  $\Omega=1$  state at  $21\,400\text{ cm}^{-1}$ .

The data in Fig. 2 can be used to determine spectroscopic parameters for this band. Because the  $f$  levels in the upper state appear to be unperturbed, it is possible to extract a value of  $\nu_0$  from the  $y$ -intercept of the line defining the  $f$  level term energies. This value is  $21\,389.7245 \pm 0.0030\text{ cm}^{-1}$ , with the slope of the line being  $0.485\,98 \pm 0.000\,13\text{ cm}^{-1}$ . This slope corresponds to the value of  $B' + \frac{1}{2}q'$ . Because the perturbation affecting the  $e$  levels depends upon  $J$ , the magnitude of the perturbation must be zero in the nonrotating molecule. This means that at  $J=0$ , both term energies must coincide at  $\nu_0$ . If it is assumed that the first two data points defining the  $F_e$  line in Fig. 2 are relatively unperturbed, these two data points, along with the  $y$ -intercept that was previously determined, can be used to extract an unperturbed  $F_e$  line. This line intersects the  $y$ -axis at the same location as the  $F_f$  line and has a slope of  $0.429\,77 \pm 0.000\,79\text{ cm}^{-1}$ . This is the value of  $B' - \frac{1}{2}q'$ . The average of the two slopes yields an unperturbed value for  $B'$  of  $0.457\,87 \pm 0.000\,80\text{ cm}^{-1}$ , and the difference between the two slopes yields a value for the lambda doubling parameter of  $q' = 0.056\,21 \pm 0.000\,80\text{ cm}^{-1}$ . Of course, this assumes that the first two data points of the  $F_e$  line are unperturbed. Because these two data points can visually be seen to very nearly extrapolate to the  $y$ -intercept determined by a fit of the  $F_f$  levels, this is a reasonably good assumption. At any rate, this procedure yields a better estimate of the spectroscopic parameters for this band than could be provided by an attempt to fit the line positions to Eq. (1).

### G. Other perturbed bands

Plots similar to that in Fig. 2 can be made for the other bands that were found to not fit well in Eq. (1). These bands, found near  $20\,870\text{ cm}^{-1}$ ,  $22\,120\text{ cm}^{-1}$ , and  $23\,090\text{ cm}^{-1}$ , have both the  $e$  and  $f$  levels perturbed, however. As such, it is impossible to extract reliable unperturbed estimates of the spectroscopic constants for these bands. Combination differences calculated for the  $20\,870\text{ cm}^{-1}$  and  $22\,120\text{ cm}^{-1}$  bands yielded values of  $B''$  reasonably close to the weighted average values tabulated in Table I, indicating that they too most likely originate from the ground state of MoC. Combination differences for the  $23\,090\text{ cm}^{-1}$  band, however, gave a considerably different value for  $B''$ , about  $0.533\text{ cm}^{-1}$ . This could be simply a result of the data obtained for this particular band being of substantially poorer quality than for the other bands in this investigation.

### H. Ionization energy

Sievers, Chen, and Armentrout have recently determined the dissociation energy of  $\text{MoC}^+$  to be  $4.31 \pm 0.20\text{ eV}$ .<sup>28</sup> Using this number along with the recently revised value for the dissociation energy of MoC ( $5.01 \pm 0.13\text{ eV}$ ) (Ref. 16) and the known ionization energy (IE) of atomic Mo ( $7.092\,43$

eV),<sup>29</sup> the ionization energy of MoC can be calculated to be  $7.79 \pm 0.24\text{ eV}$ . An attempt was made to determine the IE of MoC more precisely by scanning the previously surveyed spectral region while employing for photoionization an excimer laser operating on a KrF gas fill to provide a  $5.00\text{ eV}$  photoionization source. When the spectral region was originally scanned using  $6.42\text{ eV}$  excimer radiation for photoionization (ArF gas fill), the bands located at  $18\,611.9526\text{ cm}^{-1}$  and  $23\,323.5623\text{ cm}^{-1}$  were determined to be the lowest and highest energy bands, respectively, that could be confirmed as originating from the vibrationless level of the ground state of MoC. A survey scan utilizing  $5.00\text{ eV}$  radiation for photoionization would have allowed the IE to be measured with no more than a  $\pm 0.06\text{ eV}$  uncertainty if the IE fell in the range  $7.31\text{--}7.89\text{ eV}$  and if no other complications were present. This determination was not possible, however, because the  $\text{MoC}^+$  ion signal produced when KrF radiation was used for photoionization could not be attenuated sufficiently to conduct an R2PI experiment. In fact, as the ionization laser was attenuated, the  $\text{Mo}^+$  signal decreased more rapidly than the molecular ion signal until no comparison was possible because the  $\text{Mo}^+$  signal was no longer detectable and the  $\text{MoC}^+$  signal continued to nearly saturate the detector. Because MoC cannot be one-photon ionized at a photon energy of  $5.00\text{ eV}$  and because atomic Mo must be nonresonantly ionized by two  $5.00\text{ eV}$  photons,<sup>29,30</sup> the only reasonable explanation for the intense  $\text{MoC}^+$  signal observed using KrF radiation is that the MoC molecule has a strong absorption that is excited at this wavelength and that absorption of a second photon then leads to an efficient ionization process. Nevertheless, an upper bound of  $8.73\text{ eV}$  for IE(MoC) can be extracted from the data collected in this study. This is consistent with the value of  $7.79 \pm 0.24\text{ eV}$  determined primarily using thermochemical data, but it does not represent an improvement in its precision.

## IV. DISCUSSION

### A. Expected trends from MF to MO to MN to MC

Through the careful work of dedicated spectroscopists, the electronic structure of many of the transition metal monoxides is now well characterized.<sup>31</sup> The insight into the bonding of these species that has been gained through this work has led to a natural tendency to apply the bonding models developed for the metal–oxygen bond to less studied systems, such as the transition metal carbides, nitrides, and fluorides. In order for the metal oxide paradigm to be directly applicable to the carbide, nitride, or fluoride of any one transition metal atom, the valence  $2s$  and  $2p$  orbitals need to be at nearly the same energy in C, N, O, and F. This is not true, however, as a quick perusal of the relevant atomic energy levels and ionization energies will indicate.<sup>30</sup> This conclusion can be illustrated more dramatically by plotting the calculated energies of the  $2s$  and  $2p$  orbitals for the  $2s^2 2p^n$  configuration for the second row atoms B, C, N, O, and F. These energies, calculated using the Hartree–Fock program supplied by Charlotte Froese Fischer,<sup>32</sup> are shown in Fig. 3. As can be seen, both the  $2s$  and  $2p$  orbital energies drop considerably from B to C to N to O to F, but it is the  $2s$

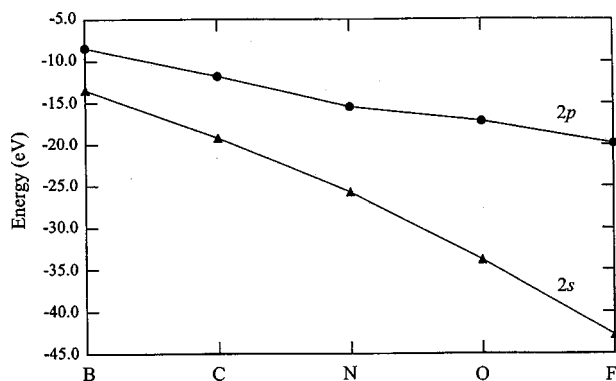


FIG. 3.  $2p$  and  $2s$  orbital energies of B, C, N, O, and F. The calculated Hartree-Fock energies of the  $2s$  and  $2p$  orbitals are shown for the  $2s^2 2p^n$  configuration across the  $2p$  series from boron to fluorine. The  $2p$  orbital energies are shown with closed circles on the upper line, and the  $2s$  orbital energies are shown with the closed triangles on the lower line. Both orbital energies drop as the nuclear charge increases, but the  $2s$  orbital drops more rapidly because it is not well shielded from the added nuclear charge by the additional  $2p$  electrons.

orbital that undergoes the most dramatic drop. This well known behavior is due to the increase in nuclear charge as one moves across the series, and the effect is greater for the  $2s$  orbital because the added  $2p$  electrons do not effectively shield the  $2s$  electrons from the added nuclear charge. Because these different ligand atoms have substantially different valence orbital energies, significant changes in the electronic structure can be expected as the oxygen ligand atom is replaced with N, C, or F. The metal oxides may, therefore, provide a misleading model for the carbides, the focus of this work.

Similar Hartree-Fock calculations carried out for the  $4d$  transition metal series to obtain the  $4d$  and  $5s$  orbital energies show that these orbitals lie between roughly  $-4$  eV and  $-14$  eV. Consequently, the drop in valence orbital energies shown in Fig. 3 for the ligand atoms causes the  $nd$  and  $(n+1)s$  valence orbitals of the transition metals to lie much closer in energy to the carbon valence orbitals than to the fluorine valence orbitals. As a consequence, the bonding orbitals in the transition metal fluorides tend to be localized primarily on the fluorine atoms while the antibonding orbitals are localized more on the metal atoms. For the metal fluorides, little M-F orbital mixing is expected, and the molecular orbitals are expected to lie very close in energy to their corresponding atomic orbitals in the separated atoms. As a result, it is expected that a grouping of the molecular orbitals into two classes will occur: (1) weakly bonding and closely spaced ligand-based orbitals that lie low in energy and (2) weakly antibonding or nonbonding and closely spaced metal-based orbitals that are generally much higher in energy. Most of the bonding interaction in the fluorides is expected to arise from the transfer of metal electrons into one of the ligand-based orbitals, leading to bonding that can best be described as ionic. The inherently closely spaced metal-based orbitals then favor high multiplicity ground states in which the electrons are placed in different orbitals to minimize electron-electron repulsions and maximize exchange stabilization. Because of the wide separation between the

bonding and antibonding orbitals in the transition metal fluorides, the higher energy spectroscopic transitions observed in the metal fluorides can be classified as charge transfer transitions in which an electron in a ligand centered orbital is moved to a metal centered orbital.

The increasingly better energetic match between the valence orbitals of the ligand atom with those of the transition metal on moving from F to O to N to C is expected to lead progressively to molecular orbitals that can be considered to share electrons more equally between the two atomic centers. The molecular orbitals of the transition metal carbides are therefore expected to be displaced further in energy from their atomic progenitors due to the greater interaction between the energetically well-matched atomic orbitals, and they are not expected to remain so closely spaced as in the fluorides. It is therefore less tenable to categorize the molecular orbitals into the two groups mentioned above and not as straightforward to identify the orbitals as ligand based or metal based in the carbides. As a consequence, these molecules are better characterized as covalent than as ionic.

From these differences in orbital structure, it is reasonable to expect that high multiplicity ground states will be more strongly favored for MF, MO, and MN species than for MC molecules. Based on the available experimental and theoretical studies, this expectation is borne out well. Of the eleven transition metal carbides that have been experimentally investigated [FeC ( $^3\Delta_i$ ),<sup>1</sup> CoC ( $^2\Sigma^+$ ),<sup>4,5</sup> NiC ( $^1\Sigma^+$ ),<sup>6</sup> YC ( $^4\Pi_i$ ),<sup>7</sup> ZrC ( $^1\Sigma^+$ ),<sup>8</sup> NbC ( $^2\Delta_r$ ),<sup>9</sup> MoC ( $^3\Sigma^-$ ), RuC ( $^1\Sigma^+$ ),<sup>12</sup> RhC ( $^2\Sigma^+$ ),<sup>13</sup> PdC ( $^1\Sigma^+$ ,  $^3\Pi$ , or possibly  $^3\Sigma^-$ ),<sup>14</sup> IrC ( $^2\Delta_i$ ),<sup>33,34</sup> and PtC ( $^1\Sigma^+$ ) (Refs. 35, 36)], only YC has a ground state multiplicity greater than 3. In contrast, numerous oxides possess ground states with multiplicities greater than 3. For example, VO ( $^4\Sigma^-$ ),<sup>31</sup> CrO ( $^5\Pi_r$ ),<sup>31</sup> MnO ( $^6\Sigma^+$ ),<sup>31</sup> FeO ( $^5\Delta_i$ ),<sup>31</sup> CoO ( $^4\Delta_i$ ),<sup>31</sup> NbO ( $^4\Sigma^-$ ),<sup>37</sup> and MoO ( $^5\Pi_r$ ),<sup>23</sup> and possibly others, possess high multiplicity ground states. Particularly demonstrative of this tendency are the sets of isoelectronic molecules MnF ( $^7\Sigma^+$ ),<sup>38</sup> FeO ( $^5\Delta$ ),<sup>31</sup> and NiC ( $^1\Sigma^+$ ) (Ref. 6) as well as CrF ( $^6\Sigma^+$ ),<sup>39-41</sup> MnO ( $^6\Sigma^+$ ),<sup>31</sup> FeN ( $^2\Delta$ ),<sup>42</sup> and CoC ( $^2\Sigma^+$ ).<sup>4,5</sup>

## B. Expected trends from YC to AgC

In the previous section, it was made clear that changing the ligand atom attached to any single transition metal from F to O to N to C to B is expected to change the nature of the bonding in the molecule considerably. For a given ligand atom, changing the metal atom has consequences as well. The added nuclear charge on moving across the  $4d$  transition metal series causes all atomic orbitals to drop in energy. In this case, however, it is the  $4d$  orbitals that drop more rapidly than the  $5s$  because the  $5s$  orbital has a greater spatial extent than the  $4d$ , and the added  $d$  electrons are effective in shielding the  $s$  electrons for this reason. This trend for the  $4d$  series is illustrated in Fig. 4 where the  $4d$  and  $5s$  Hartree-Fock<sup>32</sup> orbital energies for the  $4d^n 5s^1$  configuration of the neutral metals have been plotted. The primary consequence of this trend across the  $4d$  transition metal series is that all the molecular orbitals with a large amount of  $4d$  character ( $2\delta$ ,  $6\pi$ , and  $13\sigma$ ) are expected to drop in energy relative to the  $12\sigma$  orbital, which is primarily  $5s$  in character,

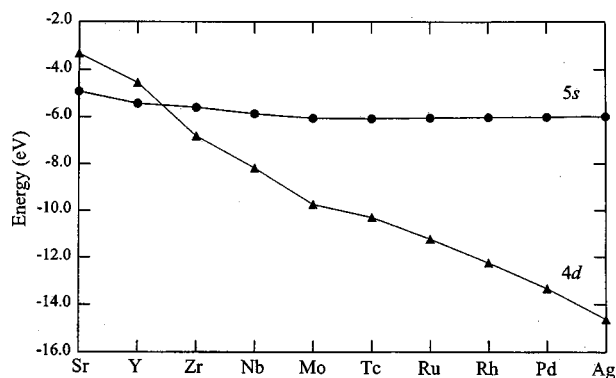


FIG. 4.  $5s$  and  $4d$  orbital energies across the  $4d$  transition metal series. The calculated Hartree-Fock energies of the  $5s$  and  $4d$  orbitals of the  $4d$  transition metals in the  $5s^1 4d^{n+1}$  configuration are shown. The  $5s$  orbital energies are shown along the line connecting the closed circles, and the  $4d$  energies are shown along the line connecting the closed triangles. The  $5s$  orbital first drops and then raises slightly in energy as the nuclear charge is increased because it is well shielded from the added nuclear charge by the additional  $4d$  electrons, which are more spatially compact than the  $5s$  orbital.

as one moves left to right across the  $4d$  series. Figure 4 suggests that in the early transition metal carbides, such as YC, all of these  $4d$ -based orbitals will lie above the  $12\sigma$  orbital, but as one moves to the right, this will no longer be the correct ordering.

The first of the  $4d$ -based orbitals to drop below the  $12\sigma$  orbital is the  $2\delta$  orbital, which is nonbonding in character. Thus, it is found that the  $12\sigma$  orbital is occupied and the  $2\delta$  orbitals are empty in the ground  $10\sigma^2 11\sigma^1 5\pi^3 12\sigma^1$ ,  $^4\Pi_i$  state of YC, clearly placing the  $2\delta$  orbital above the  $12\sigma$  orbital. By the time NbC is reached, however, this situation is reversed, and the  $2\delta$  orbital is occupied while the  $12\sigma$  orbital is empty in the  $10\sigma^2 11\sigma^2 5\pi^4 2\delta^1$ ,  $^2\Delta_r$  ground state. Between YC and NbC the energy ordering of the  $12\sigma$  and  $2\delta$  orbitals is reversed, a result that is a direct consequence of the orbital energy trends depicted in Fig. 4 for the isolated metal atoms.

### C. The $X^3\Sigma^-(0^+)$ ground state of MoC

Now that the trends expected as the ligand atom is changed and as the metal atom is changed have been discussed, it is possible to understand the ground state electronic structure of MoC. In Fig. 5 is shown a molecular orbital diagram that will prove useful in determining the ground state orbital configuration of MoC. The character of the  $10\sigma$  orbital is mainly C  $2s$  while the  $11\sigma$  and  $5\pi$  orbitals are strongly bonding combinations of the metal centered  $4d\sigma$  and  $4d\pi$  orbitals with the carbon  $2p\sigma$  and  $2p\pi$  orbitals, respectively. The energetic ordering of the  $11\sigma$  and  $5\pi$  orbitals is chosen to be consistent with the ordering suggested by the calculations of Shim and Gingerich.<sup>16</sup> The  $13\sigma$  and  $6\pi$  molecular orbitals are the antibonding counterparts to the bonding  $11\sigma$  and  $5\pi$  orbitals. The  $2\delta$  orbital is almost purely metal  $4d\delta$  in character. The  $12\sigma$  orbital is most likely nonbonding in character and composed mainly of the metal  $5s$  orbital, as is demonstrated from the hyperfine splittings analyzed in the RuC molecule.<sup>12</sup>

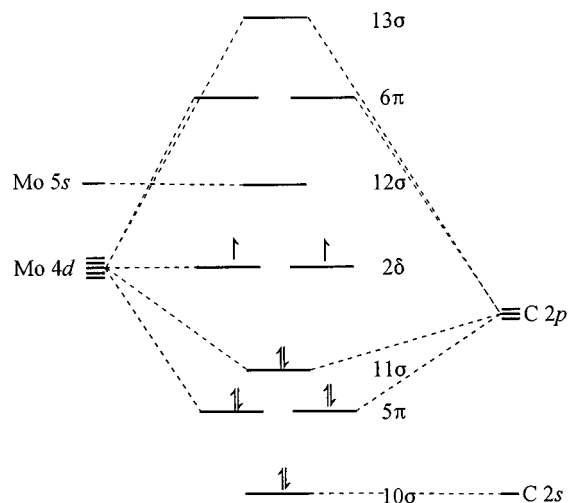


FIG. 5. Qualitative molecular orbital diagram for MoC. The  $10\sigma$  orbital is mainly a carbon  $2s$  orbital. The  $11\sigma$  and  $5\pi$  orbitals are bonding combinations formed from the molybdenum  $4d\sigma$  and  $4d\pi$  orbitals with the carbon  $2p\sigma$  and  $2p\pi$  orbitals, and the  $13\sigma$  and  $6\pi$  orbitals are the corresponding antibonding combinations. The  $2\delta$  orbital is a nonbonding orbital formed from the molybdenum  $4d\delta$  orbitals. Finally, the  $12\sigma$  orbital is largely nonbonding in character and composed mainly of the  $5s$  character on molybdenum. The orbital occupations for the  $^3\Sigma^-(0^+)$  ground state are illustrated here.

All rotationally resolved bands observed in this study of MoC fit as  $\Omega = 1 \leftarrow 0$  transitions. It was necessary to include lambda doubling to achieve satisfactory fits, but all lines were simply undoubled  $P(J)$ ,  $R(J)$ , and  $Q(J)$  lines. These facts, taken together, imply that the ground state of MoC must be a single  $\Omega = 0$  state rather than an  $\Omega = 0^\pm$  pair such as might result from a  $^3\Pi$  state. This further implies that the ground state must be a  $\Sigma$  state. If the 10 valence electrons of MoC are placed into the molecular orbitals in Fig. 5, the final two electrons can be placed in a number of locations. First, the two electrons can be placed in the  $2\delta$  orbitals such that they are high spin coupled to yield a  $^3\Sigma^-(0^+)$  ground state. The  $^1\Sigma^+(0^+)$  term arising from this  $2\delta^2$  configuration is not expected to emerge as the ground state because of unfavorable exchange interactions. If the ordering of the  $12\sigma$  and  $2\delta$  orbitals were reversed, a possible ground state of  $^1\Sigma^+(0^+)$  could arise from a  $12\sigma^2$  configuration. If these two molecular orbitals were sufficiently close in energy, a  $^3\Delta$  ground state would be likely, but it has already been established that the ground state must be a  $\Sigma$  state. Establishing the ground state of MoC is now reduced to an informed choice between the  $2\delta^2$ ,  $^3\Sigma^-(0^+)$  and the  $12\sigma^2$ ,  $^1\Sigma^+(0^+)$  possibilities.

Recent *ab initio* calculations on MoC and experimental results for the surrounding  $4d$  transition metal carbides can assist in making this choice. As has been mentioned, the ground state of YC is  $^4\Pi$ ,  $10\sigma^2 11\sigma^1 5\pi^3 12\sigma^1$ . The last occupied molecular orbital is the  $12\sigma$  orbital. The  $12\sigma$  orbital lies below the  $2\delta$  in this case, a situation analogous to the fact that the  $5s$  orbital of Y lies below the  $4d$  orbitals. As this paper goes to press, ZrC is undergoing spectroscopic scrutiny in the laboratory of Professor A. J. Merer.<sup>8</sup> There are several possibilities for the ground state. If the bonding interaction between the metal and carbon atoms becomes

great enough at Zr, ZrC may be forced into the  $10\sigma^2 11\sigma^2 5\pi^4$ ,  $^1\Sigma^+$  ground term. On the other hand, if the bonding interaction does not change much on moving from YC to ZrC, and the  $11\sigma$  orbital remains only poorly bonding, two other possibilities are a  $10\sigma^2 11\sigma^1 5\pi^4 12\sigma^1$ ,  $^3\Sigma^+$  ground state that might emerge if the  $12\sigma$  orbital lies lower than the  $2\delta$  orbital and a  $10\sigma^2 11\sigma^1 5\pi^4 2\delta^1$ ,  $^3\Delta_r$  ground state that may emerge if the  $12\sigma$  and  $2\delta$  orbitals lie in the order  $2\delta < 12\sigma$ . The spectra support the  $^1\Sigma^+$  ground state at this point.

At NbC the ground state is  $^2\Delta_r$ ,  $10\sigma^2 11\sigma^2 5\pi^4 2\delta^1$ . At this point the metal  $4d$  orbitals lie below the  $5s$  orbital, allowing the  $^2\Delta$  term to arise as the ground state rather than the  $^2\Sigma^+$  term. Figure 4 illustrates that the energy of the  $4d$  orbitals continues to drop across the series. Because of this, it seems likely that once the  $2\delta$  orbital has been filled with a single electron in NbC it will continue to be filled upon moving to MoC. It is not reasonable to expect that the  $12\sigma$  orbital should be doubly occupied at MoC when the  $4d$  orbitals have dropped so far below the  $5s$  in energy. This makes it almost certain that the ground state of MoC is  $^3\Sigma^-$ . In support of this claim is the recent *ab initio* relativistic CASSCF calculation by Shim and Gingerich<sup>16</sup> that shows the  $^3\Sigma^-$  term to be the ground state by approximately  $4500\text{ cm}^{-1}$ .

Now that the ground state of MoC has been determined, it is possible to extend the trend to comment on a carbide that, understandably, is not likely to be studied in the near future: TcC. There are two possible ground states for this molecule. The first is  $^2\Delta_i$  deriving from the  $2\delta^3$  configuration, and the second is a higher spin  $^4\Sigma^-$ ,  $2\delta^2 12\sigma^1$  possibility. If the  $4d$  orbitals drop sufficiently between Mo and Tc to allow TcC to recoup the loss of exchange energy and to pay the price of additional electron–electron repulsion, the  $^2\Delta$  term will emerge as the ground state. Otherwise, the high multiplicity  $^4\Sigma^-$  term will be the ground state.

The trend can be continued to other  $4d$  transition metal carbides for which the ground state is known. After TcC comes RuC with a ground state of  $^1\Sigma^+$ ,  $2\delta^4$ . At RuC, the  $4d$  orbitals, and consequently the  $2\delta$  molecular orbitals, have dropped sufficiently in energy that the added electron–electron repulsion occurring in the  $2\delta^4$ ,  $^1\Sigma^+$  state as compared to the  $2\delta^3 12\sigma^1$ ,  $^3\Delta_i$  state can be entirely recouped. Rhodium carbide<sup>13</sup> continues the trend by beginning the process of filling the  $12\sigma$  orbital. Its ground state is  $^2\Sigma^+$ ,  $2\delta^4 12\sigma^1$ . The ground state of PdC (Ref. 14) is  $\Omega=0^+$ , but it is unknown at this point if this results from a  $12\sigma^2$ ,  $^1\Sigma^+$  state, as would first be thought, from a  $2\delta^4 12\sigma^1 6\pi^1$ ,  $^3\Pi_0$  state, or a  $2\delta^4 6\pi^2$ ,  $^3\Sigma^-$  state that might be favored because of the unusual stability of the Pd  $4d^{10} 5s^0$  ground state configuration.<sup>30</sup> This latter possibility would imply that at Pd both the  $2\delta$  and the  $6\pi$  orbitals have dropped below the  $12\sigma$  orbital in energy. Such a possibility is not unreasonable because the increase in bond length from RhC to PdC is about  $0.1\text{ \AA}$ .<sup>14</sup> This increase is more than expected from experience with the other transition metal carbides, and it suggests that the nominally antibonding  $6\pi$  orbital may be occupied in PdC.

The rotationally resolved bands investigated here yielded

a set of lower state rotational constants, either by a direct fit to Eq. (1) or by combination differences, that appeared to be statistically the same. Because of this, it has been argued that all of the observed transitions originate from the same lower state and that any low-lying excited states lie far in energy above the ground state and are not thermally populated under our experimental conditions. Because the ground state is well separated from other electronic states, it might be thought that it would be free of perturbations from nearby states. It is possible, however, that the  $\Omega=1$  component of the ground  $^3\Sigma^-$  term may be sufficiently close to the  $\Omega=0^+$  ground component for spin-uncoupling interactions to distort the measured rotational constant from a value that is directly related to the moment of inertia, thereby introducing errors into the calculated ground state bond length. Similar caveats concerning heterogeneous perturbations by relatively remote states apply to all the excited states observed in this investigation, where the importance of such rotationally dependent perturbations is manifested by the lambda doubling observed in the  $\Omega'=1$  upper states. In the ground  $\Omega=0^+$  state, however, heterogeneous perturbations are more insidious because they can distort the rotational constant from a value that is related to the moment of inertia without revealing their presence. No lambda doubling is possible in the  $\Omega=0^+$  ground state to warn the investigator that something is amiss.

A  $^3\Sigma^-$  term is composed of two  $\Omega$  levels,  $0^+$  and  $1$ . If these two components are not well separated in energy, as might be expected by the absence of first order spin–orbit interactions, they will be thoroughly mixed by the  $S$ -uncoupling operator such that it becomes invalid to consider the ground state as belonging to Hund's case (a). It would be more properly described in a Hund's case (b) basis. It was possible to fit rotational line positions for MoC assuming Hund's case (a) applied to the ground state; therefore, the two components must be separated by a second order spin–orbit effect. The most likely source of such an effect is interaction with the  $^1\Sigma^+$  state that derives from the same  $2\delta^2$  configuration as the ground  $^3\Sigma^-$  state. The off-diagonal spin–orbit matrix element coupling the  $^1\Sigma^+(0^+)$  and  $^3\Sigma^-(0^+)$  states can be readily estimated using the tabulated spin–orbit parameters for atomic Mo ( $\zeta_{\text{Mo},4d}=677\text{ cm}^{-1}$ ),<sup>26</sup> assuming that the  $2\delta$  molecular orbitals are purely Mo  $4d$  in character. Further, if the separation between the  $^1\Sigma^+(0^+)$  and  $^3\Sigma^-(0^+)$  states is taken from the *ab initio* work of Shim *et al.* as  $11\,639\text{ cm}^{-1}$ ,<sup>16</sup> the separation of the two  $^3\Sigma^-$  components can be predicted to be  $155.4\text{ cm}^{-1}$  from a diagonalization of the  $2\times 2$  matrix problem. Employing the rotational Hamiltonian derived for a  $^3\Sigma^-$  state by Hougen,<sup>43</sup> it may be estimated that the measured value of  $B''$  has been reduced by  $0.008\,12\text{ cm}^{-1}$  by the spin-uncoupling interaction. Making this correction to  $B''$  we find that our estimate of the ground state bond length,  $r_0$ , is changed from  $1.6877\text{ \AA}$  to  $1.6755\text{ \AA}$ . This is not a negligible correction.

The uncertainty in the exact position of the  $^1\Sigma^+$  state and the lack of any direct observation of the  $\Omega=0^+$ ,  $\Omega=1$  splitting in the  $^3\Sigma^-$  state precludes any precise correction to the measured rotational constants in Table I. The calculation above does illustrate, however, that the interaction may affect the value of  $B''$  such that it is no longer

directly related to the moment of inertia of MoC. In the absence of additional data, the value of  $r_0 = 1.6755 \text{ \AA}$  obtained above represents our best estimate of the true bond length of the MoC molecule. Nevertheless, this value will require revision when the separation between the  $\Omega = 0^+$  and 1 components of the  $X^3\Sigma^-$  ground state is accurately measured.

#### D. The MoC excited state manifold from 17 700 $\text{cm}^{-1}$ to 24 000 $\text{cm}^{-1}$

If the selection rules appropriate to Hund's case (a) are to be followed ( $\Delta\Sigma = 0$ ,  $\Delta S = 0$ ,  $\Delta\Lambda = \pm 1, 0$ , and  $\Delta\Omega = \pm 1, 0$ ), only  $^3\Pi_1$  and  $^3\Sigma_0^-$  states can be accessed from the ground  $^3\Sigma_0^-$  term. Because of the spin-orbit contamination of the ground  $2\delta^2$ ,  $^3\Sigma_0^-$  term by the  $2\delta^2$ ,  $^1\Sigma_0^+$  term, however, transitions to  $^1\Pi_1$  and  $^1\Sigma_0^+$  states are also possible and need to be given consideration. Therefore, any upper states which are observed in transitions from the ground  $^3\Sigma_0^-$  term must be observed because they possess  $^3\Pi_1$ ,  $^3\Sigma_0^-$ ,  $^1\Pi_1$ , or  $^1\Sigma_0^+$  character in their electronic wave functions. Because all of the upper states observed in the range from 17 700 to 24 000  $\text{cm}^{-1}$  have  $\Omega = 1$ , we may conclude that they are made allowed by spin-orbit mixing with either a  $^3\Pi_1$  or a  $^1\Pi_1$  state. *Ab initio* calculations<sup>16</sup> have placed a  $^3\Pi_1$  state at about 15 500  $\text{cm}^{-1}$ , near the region probed in this study. This state is calculated to derive from the excitation of a  $5\pi$  electron to the  $12\sigma$  orbital, leading to an electronic configuration of  $10\sigma^2 11\sigma^2 5\pi^3 2\delta^2 12\sigma^1$ ,  $^3\Pi$ . There are, of course, too many vibronic transitions observed to be accounted for by just one electronic state. The states with which the  $^3\Pi_1$  state can mix via the spin-orbit interaction include  $^1,5\Pi_1$ ,  $^3,5\Delta_1$ ,  $^3,5\Sigma_1$ , and other  $^3\Pi_1$  states. There are, then, a wide range of states that can gain intensity in transitions from the ground state by interaction with this (or other)  $^3\Pi_1$  states. Unfortunately, the one available *ab initio* calculation is of little help in deducing the likely energies of these possible states. In any case, it seems that significant spin-orbit mixing among a number of states is probably responsible for the general complexity of the MoC vibronic spectrum.

The question still remains as to why there are no directly observed  $\Omega = 0$  states. As deduced above, any  $\Omega = 0$  upper states can only be observed to the extent that  $^3\Sigma_0^-$  or  $^1\Sigma_0^+$  character is mixed into their electronic wave functions. The fact that there are no observed  $\Omega = 0$  states in the investigated energy range implies that there must be no  $^3\Sigma^-$  or  $^1\Sigma^+$  states in this region which are optically connected to the  $2\delta^2$ ,  $^3\Sigma_0^-$  or  $2\delta^2$ ,  $^1\Sigma_0^+$  terms. Based upon the *ab initio* calculations by Shim,<sup>16</sup> the lowest energy excited configuration that generates a  $^3\Sigma^-$  state results from the excitation of a bonding  $11\sigma$  electron to the nonbonding  $12\sigma$  orbital. Shim calculates that the  $^5\Sigma^-$  state deriving from this  $10\sigma^2 11\sigma^1 5\pi^4 2\delta^2 12\sigma^1$  configuration lies at 6178  $\text{cm}^{-1}$ . The  $^3\Sigma^-$  term coming from this same configuration will lie higher in energy but probably still considerably below the range of energies investigated here. To higher energies one expects to find  $^3\Sigma^-$  terms deriving from the excitation of a  $5\pi$  electron to a  $6\pi$  orbital, as well as from the excitation of an  $11\sigma$  electron to the  $13\sigma$  orbital. These represent bonding

to antibonding excitations, however, and presumably occur at energies somewhat above the range of energies probed in our experiments. Based on these ideas, it may be possible to directly observe  $\Omega = 0$  states if the regions to the red or blue of the current study are investigated. This is beyond the scope of the present investigation, however.

#### V. CONCLUSION

In this study there was considerable difficulty interpreting the excited electronic manifold of MoC, but the ground state was successfully characterized as the  $\Omega = 0^+$  component of a  $^3\Sigma^-$  term resulting from the  $10\sigma^2 11\sigma^2 5\pi^4 2\delta^2$  configuration. It appears to be well isolated from any other electronic state such that it adheres strongly to Hund's case (a), although a minor admixture of the  $10\sigma^2 11\sigma^2 5\pi^4 2\delta^2$   $^1\Sigma^+$  term is undoubtedly present and responsible for the splitting into  $\Omega = 0^+$  and  $\Omega = 1$  components. Unfortunately, the  $\Omega = 1$  component of this state was not observed, making it impossible to rigorously correct the measured ground state rotational constant,  $B_0$ , to obtain a true ground state bond length,  $r_0$ . Employing theoretical estimates of the location of the  $^1\Sigma^+$  term, our best estimate of the true value of  $r_0$  is 1.6755  $\text{Å}$ . There is good agreement between the theoretically predicted  $r_e$  of 1.688  $\text{Å}$  (Ref. 16) and this estimate.

The spectrum of MoC between 17 700 and 24 000  $\text{cm}^{-1}$  has proven to be difficult to interpret with any degree of satisfaction. The identification of the three band systems, with origins near 18 611, 22 520, and 20 700  $\text{cm}^{-1}$ , was far from clear. They represent, more than anything, the best attempt to make sense of a confusing array of bands spread almost higgledy-piggledy throughout the investigated region. More bands have been left unclassified than would be liked. This is undoubtedly the result of significant spin-orbit mixing between the various excited electronic states in this region. Nevertheless, the observation that all the observed bands possess  $\Omega' = 1$  demonstrates that the source of oscillator strength in the energy range probed here is a  $^3\Pi_1$  or  $^1\Pi_1$  term. A consideration of the expected electronic structure of the molecule suggests that upper states with  $\Omega = 0^+$  should be observable both to the red and blue of the probed region, where transitions corresponding to  $12\sigma \leftarrow 11\sigma$  and  $6\pi \leftarrow 5\pi$  electronic promotions, respectively, are expected.

#### ACKNOWLEDGMENTS

We thank both the U.S. Department of Energy (DE-FG03-93ER143368) and the donors of the Petroleum Research Fund, administered by the American Chemical Society, for support of this research. The authors would also like to heartily thank Professor Tim Steimle for his gift of the isotopically pure  $^{130}\text{Te}$  and sealed absorption cell used to calibrate the rotationally resolved spectra collected here. Without such generosity, this study would have been much more difficult to complete. We also thank Professor Tim Steimle and Dr. Benoit Simard for helpful comments concerning this manuscript.

- <sup>1</sup>W. J. Balfour, J. Cao, C. V. V. Prasad, and C. X. W. Qian, *J. Chem. Phys.* **103**, 4046 (1995).
- <sup>2</sup>M. D. Allen, T. C. Pesch, and L. M. Ziurys, *Astrophys. J.* **472**, L57 (1996).
- <sup>3</sup>D. J. Brugh and M. D. Morse, *J. Chem. Phys.* **107**, 9772 (1997).
- <sup>4</sup>M. Barnes, A. J. Merer, and G. F. Metha, *J. Chem. Phys.* **103**, 8360 (1995).
- <sup>5</sup>A. G. Adam and J. R. D. Peers, *J. Mol. Spectrosc.* **181**, 24 (1997).
- <sup>6</sup>D. J. Brugh and M. D. Morse (in preparation).
- <sup>7</sup>B. Simard, P. A. Hackett, and W. J. Balfour, *Chem. Phys. Lett.* **230**, 103 (1994).
- <sup>8</sup>A. J. Merer and J. R. D. Peers, Ohio State 53rd International Symposium on Molecular Spectroscopy, RI04, 1998, p. 249 (unpublished).
- <sup>9</sup>B. Simard, P. I. Presunka, H. P. Looock, A. Bércecs, and O. Launila, *J. Chem. Phys.* **107**, 307 (1997).
- <sup>10</sup>R. Scullman and B. Thelin, *Phys. Scr.* **3**, 19 (1971).
- <sup>11</sup>R. Scullman and B. Thelin, *Phys. Scr.* **5**, 201 (1972).
- <sup>12</sup>J. D. Langenberg, R. S. DaBell, L. Shao, D. Dreessen, and M. D. Morse, *J. Chem. Phys.* **109**, 7863 (1998), following paper.
- <sup>13</sup>B. Kaving and R. Scullman, *J. Mol. Spectrosc.* **32**, 475 (1969).
- <sup>14</sup>J. D. Langenberg and M. D. Morse (in preparation).
- <sup>15</sup>S. K. Gupta and K. A. Gingerich, *J. Chem. Phys.* **74**, 3584 (1981).
- <sup>16</sup>I. Shim and K. A. Gingerich, *J. Chem. Phys.* **106**, 8093 (1997).
- <sup>17</sup>Z. Fu, G. W. Lemire, Y. M. Hamrick, S. Taylor, J.-C. Shui, and M. D. Morse, *J. Chem. Phys.* **88**, 3524 (1988).
- <sup>18</sup>G. W. Lemire, G. A. Bishea, S. A. Heidecke, and M. D. Morse, *J. Chem. Phys.* **92**, 121 (1990).
- <sup>19</sup>S. Gerstenkorn and P. Luc, *Atlas du Spectre d'Absorption de la Molécule d'Iode entre 14 800–20 000 cm<sup>-1</sup>* (CNRS, Paris, 1978).
- <sup>20</sup>S. Gerstenkorn and P. Luc, *Rev. Phys. Appl.* **14**, 791 (1979).
- <sup>21</sup>J. Cariou and P. Luc, *Atlas du Spectre d'Absorption de la Molécule de Tellure entre 18 500–23 800 cm<sup>-1</sup>* (CNRS, Paris, 1980).
- <sup>22</sup>P. DeBièrre, M. Gallet, N. E. Holden, and I. L. Barnes, *J. Phys. Chem. Ref. Data* **13**, 809 (1984).
- <sup>23</sup>Y. M. Hamrick, S. Taylor, and M. D. Morse, *J. Mol. Spectrosc.* **146**, 274 (1991).
- <sup>24</sup>G. Herzberg, *Spectra of Diatomic Molecules*, reprint of 2nd ed. (Krieger, Malabar, 1989).
- <sup>25</sup>J. M. Brown and A. J. Merer, *J. Mol. Spectrosc.* **74**, 488 (1979).
- <sup>26</sup>H. Lefebvre-Brion and R. W. Field, *Perturbations in the Spectra of Diatomic Molecules* (Academic, Orlando, 1986).
- <sup>27</sup>See AIP Document No. PAPS-JCPSA6-109-013842-30 for 24 pages of absolute line positions and 6 pages of extracted spectroscopic constants. Order by PAPS number and journal reference from the American Institute of Physics, Physics Auxiliary Publication Service, 500 Sunnyside Boulevard, Woodbury, NY 11797-2999. Fax: 516-576-2223, e-mail: paps@aip.org. The price is \$1.50 for each microfiche (48 pages) or \$5.00 for photocopies up to 30 pages, and \$0.15 for each additional page over 30 pages. Airmail additional. Make checks payable to the American Institute of Physics.
- <sup>28</sup>M. R. Sievers, Y.-M. Chen, and P. B. Armentrout, *J. Chem. Phys.* **105**, 6322 (1996).
- <sup>29</sup>D. M. Rayner, S. A. Mitchell, O. L. Bourne, and P. A. Hackett, *J. Opt. Soc. Am. B* **4**, 900 (1987).
- <sup>30</sup>C. E. Moore, *Atomic Energy Levels*, Natl. Bur. Stand. U.S. Circ. 467 (U.S. GPO, Washington, D. C., 1971).
- <sup>31</sup>A. J. Merer, *Annu. Rev. Phys. Chem.* **40**, 407 (1989).
- <sup>32</sup>C. F. Fischer, *The Hartree-Fock Method for Atoms* (Wiley, New York, 1977).
- <sup>33</sup>K. Jansson and R. Scullman, *J. Mol. Spectrosc.* **36**, 268 (1970).
- <sup>34</sup>A. J. Marr, M. E. Flores, and T. C. Steimle, *J. Chem. Phys.* **104**, 8183 (1996).
- <sup>35</sup>T. C. Steimle, K. Y. Jung, and B.-Z. Li, *J. Chem. Phys.* **102**, 5937 (1995).
- <sup>36</sup>O. Appelblad, R. F. Barrow, and R. Scullman, *Proc. Phys. Soc. London* **91**, 261 (1967).
- <sup>37</sup>K. P. Huber and G. Herzberg, *Constants of Diatomic Molecules* (Van Nostrand Reinhold, New York, 1979).
- <sup>38</sup>O. Launila, B. Simard, and A. M. James, *J. Mol. Spectrosc.* **159**, 161 (1993).
- <sup>39</sup>R. Koivisto, S. Wallin, and O. Launila, *J. Mol. Spectrosc.* **172**, 464 (1995).
- <sup>40</sup>O. Launila, *J. Mol. Spectrosc.* **169**, 373 (1995).
- <sup>41</sup>V. M. Dubov and E. A. Shenyavskaya, *Opt. Spektrosk.* **62**, 195 (1987).
- <sup>42</sup>M. R. A. Blomberg and P. E. M. Siegbahn, *Theor. Chim. Acta* **81**, 365 (1992).
- <sup>43</sup>J. T. Hougen, *The Calculation of Rotational Energy Levels and Rotational Line Intensities in Diatomic Molecules* (U.S. GPO, Washington, D.C., 1970).